

Comparison of B-F and FVP inelastic collision cross sections 8

Hans Bichsel

December 18, 2008

e-mail: hbichsel@u.washington.edu

Center for Experimental Nuclear Physics and Astrophysics

Box 354290 University of Washington

Seattle, WA 98195-4290

1 Introduction

In particle physics the interactions of high speed particles along *tracks* in matter produce the effects needed to observe the particles. In most applications, the well known average quantities *stopping power* and *range* are not sufficient to describe the properties of the tracks. For a deeper understanding detailed simulations of the collisions along particle tracks with Monte Carlo (“MC”) simulations must be made [1].

A detailed description of the collision processes and the spectrum of energy losses must be known. As a preliminary description, *straggling functions* can be considered [2].¹ A discussion of the calculation of straggling functions can be found in [1, 2]. To calculate such functions *collision cross sections* differential in energy loss (DCCS) must be known. For this note only inelastic collisions of the particles (mass M) with *electrons* (mass m) in the absorber are considered [1]. Many methods to obtain inelastic collision cross sections have been described. At present we believe that the description based on the direct Coulomb interaction and on the exchange of virtual photons between the incident particles and the absorber is plausible [5, 6]. For this method we need photon absorption cross sections.

¹The functions frequently are labeled *Landau functions* [3]. For present purposes I want to restrict this expression to the specific function given in [3, 4].

Here I want to compare two methods which use different approaches for one aspect of the problem. The first one I call the Bethe-Fano method (B-F) described in Sect. 2.1 (more details are given in Sect. 2.3 of [6]). The second one is the Fermi-virtual-photon method (FVP) using the approximation for the generalized oscillator strength (GOS) shown in Fig. 1. It is described in Sect. 2.2.²

2 Methods for calculating collision cross sections

In inelastic collisions, particles with speed $v = \beta c$ lose energy E in random collisions. Large energy losses can be approximated as collisions with single electrons in the absorber, see Eq. (5). Otherwise the binding of the electrons in the atoms (or molecules) must be taken into account. For condensed matter, the outer electrons of large groups of atoms must be considered as a *collective* of electrons, Fig. 6 in Bohr's review [8].³ Associated with the energy loss E there is a *momentum transfer* q . In a classical description q depends on the instantaneous velocity u of the electron in the atom [10].

The probability of the occurrence of a momentum transfer $q = Ka_0$ for a given energy loss E is shown in Fig. 1. For a *free electron* the quantity⁴

$$Q(1 + Q/mc^2) = q^2/2m \quad (1)$$

is equal to the energy loss E [6]. For current purposes it is useful to distinguish several domains of energy loss E and momentum transfer q . In addition *longitudinal* and *transverse* collisions are considered separately, Eq. 16 in [6].

2.1 Bethe-Fano method (B-F)

Fano [6] gave the equation for the collision of a particle with speed $v = \beta c$ with an atom as a cross section doubly differential in energy loss E and momentum transfer q (represented here by Q , Eq.(1)).

$$\sigma(E, Q) = k_R Z \left[\frac{|F(E, \mathbf{q})|^2}{Q^2(1 + Q/2mc^2)^2} + \frac{|\beta_t G(E, \mathbf{q})|^2}{Q^2(1 + Q/2mc^2) - E^2/2mc^2} \right] (1 + Q/mc^2) \quad (2)$$

²This method is known by many other names: Weizsaecker-Williams method, PAI, etc. The discussion given here is based on the paper by Allison and Cobb [7] who use the expression *PAI*, but the label FVP is used here anyway. This is misleading to some extent because the B-F method also uses virtual photons.

³Further details can be found in [9] and in Sect. 2.10 of Fano.

⁴See Sect. II.A in [15].

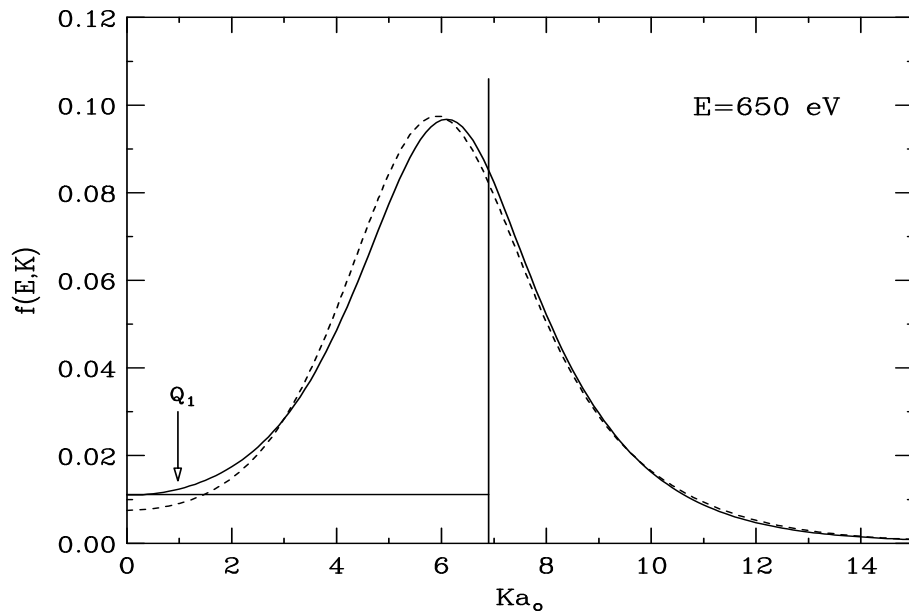


Figure 1: Generalized oscillator strength $f(E, K)$ for Si for an energy transfer $E = 650$ eV to the 2p-shell electrons [2]. Solid line: calculated with Herman-Skilman potential [19], dashed line: hydrogenic approximation [12]. The horizontal and vertical line define the FVP approximation (Sect. 2.2). The upper limit for the integral of Eq. (10) is Q_1 . See Figs. 3-8 in [2] for more detail.

where $k_R = 2\pi z^2 e^4 / (mc^2 \beta^2)$, $|F(E, \mathbf{q})|^2$ represents the interaction matrix element for longitudinal excitations, and $|G(E, \mathbf{q})|^2$ represents that for transverse excitations.

2.1.1 Approximate expressions

For small particle speeds, $\beta_t \ll 1$, and momentum transfers $Q_M \ll 2mc^2$, a non-relativistic approximation can be used

$$\sigma(E, Q) = k_R \frac{Z}{Q^2} |F(E, \mathbf{q})|^2 = k_R \frac{Z}{EQ} f(E, Q) \quad (3)$$

where

$$f(E, Q) \equiv \frac{E}{Q} |F(E, \mathbf{q})|^2 \quad (4)$$

is called the *generalized oscillator strength* GOS [20].⁵

For free electrons the quantities E and Q are the same, and Eq. (3) can be written as the *Rutherford*

⁵In Fano's use, $\int f(E, 0) dE = 1$.

cross section

$$\sigma_R(E; \beta) = k_R \frac{1}{E^2}, \quad k_R = \frac{z^2}{\beta^2} 2.54955 \cdot 10^{-19} \text{ eVcm}^2. \quad (5)$$

Since a single free electron is involved, $f(E, Q)=1$.

Note that \mathbf{q} gives the change in direction of the velocity of the incident particle, but gives at best qualitative information about the direction of the velocity of the secondary electron produced in the collision because a fraction of q is transferred to the residual ion [16, 17].

2.1.2 Generalized oscillator strength GOS

To calculate $\sigma(E, Q)$ we need to calculate first the matrix elements $F_n(q)$ and $G_n(q)$ given by Eq. 2 (Eq. 17 in [6]). Analytic expressions calculated with hydrogenic wavefunctions can be found in [11, 12, 13, 14]. A comprehensive discussion is given in [15], in particular the functions $f(E, Q)$ are shown. A method based on the use of a *Hartree-Slater* central field model of the atom has been described by Manson [19, 20]. Results from a more detailed study, using this approach, are given in [2, 21]. Other methods to calculate $f(E, Q)$ have been described [7, 22, 23, 24, 25]. A comprehensive study has been made by Bote and Salvat [18]. Examples of different approximations of GOS are shown in Fig. 1.

2.1.3 Singly differential cross sections

For many applications details about the momentum transfer q are not needed. The *singly differential cross sections* (DCCS) $\sigma_b(E; \beta)$ for energy losses E can then be used for the simulations

$$\sigma_b(E; \beta) = \int_{Q_m}^{\infty} \sigma(E, Q) dQ \quad (6)$$

where $Q_m = E^2/(2mc^2\beta^2)$. Note that $f(E, Q)$ converges to zero for large q , Fig. 1. The dependence on particle speed is only through Q_m .⁶

⁶If the mean value of E (equivalent to the *stopping power*) only is needed, it can be calculated with [6, 15, 21]

$$M_1(\beta) = \int E dE \int_{Q_m}^{Q_M} \sigma(E, Q) dQ \quad (7)$$

where $Q_m \sim E^2/Q_M$, $Q_M \sim 2mc^2\beta^2$ and the dependence on particle speed β only appears in Q_m and Q_M . Some calculations of M_1 with the approximation of GOS given in [19] have been made [26]. I calculated stopping powers for Al and Si with this method [21].

From Fig. 1 it can be seen that the GOS for small K can be approximated by the value of $f(E, 0)$, i.e. the dipole oscillator strength DOS which is related to the optical absorption cross section $\sigma_\gamma(E)$ by [27]

$$\sigma_\gamma(E) = \frac{\pi e^2 \hbar}{mc} f(E, 0). \quad (8)$$

I am aware of only one paper in which the full calculation of $\sigma(E; \beta)$ with the approximation of GOS given in [19] has been made [2]. For numerical calculations it is practical to separate the integral over Q in Eq. (6) into several parts.⁷ For the B-F program used here three ranges are used, giving the functions $\sigma_1(E; \beta)$, $\sigma_2(E; \beta)$ and $\sigma_3(E; \beta)$. A fourth function $\sigma_4(E; \beta)$ is needed to calculate the solid state collisions.

The several parts are itemized next.

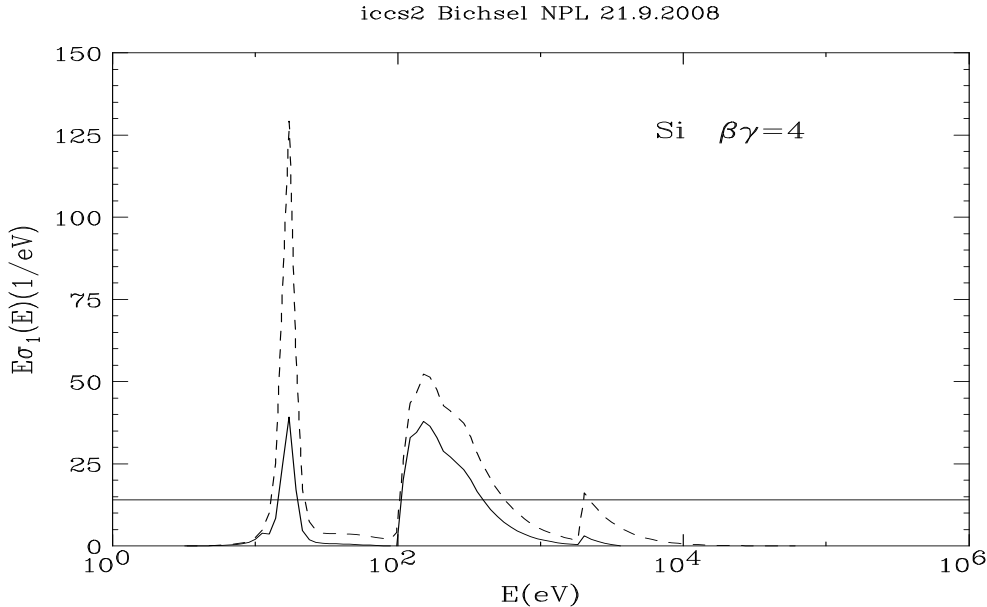


Figure 2: Solid line: first part of B-F cross section, given by Eq.(10), for $\beta\gamma = 4$, $\beta \sim 0.97$. Note that functions for greater $\beta\gamma$ will be only slightly larger. Dashed line: corresponding part of FVP cross section, Eq.(17). Horizontal line: Rutherford cross section for $Z = 14$ electrons. The functions are multiplied by E^2/k_R or $E^2\beta^2\pi/\alpha$.

⁷The tables of $f(E, Q)$ used for [21] amounted to 200 MB, which was a large number on a PC in 2001.

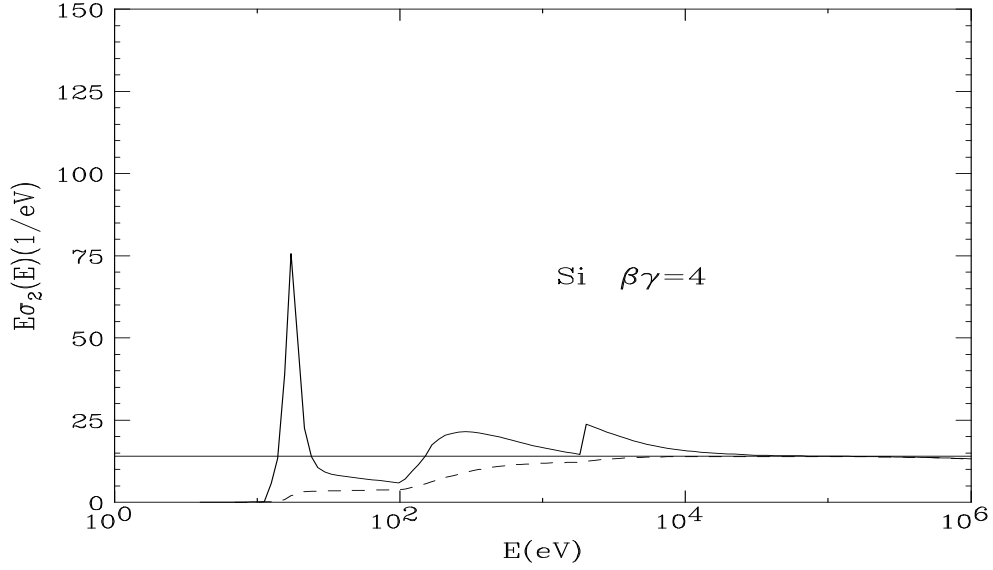


Figure 3: Second and third part of B-F cross section, Eqs. (11,12), solid line; corresponding part of FVP, given by Eq.(18): dashed line. Horizontal line: Rutherford cross section for $Z = 14$ electrons. The $\sigma(E)$ are multiplied by E^2/k_R or $E^2\beta^2\pi/\alpha$.

- For small Q , approximate $f(E, Q)$ by $f(E, 0)$ in Eq. (2) and then use Eq. (6) for the interval $Q_m < Q < Q_1$

$$\sigma_1(E; \beta) = \int_{Q_m}^{Q_1} \sigma(E, 0) dQ = k_R \frac{Z}{E} f(E, 0) \int_{Q_m}^{Q_1} \frac{1}{Q} dQ = \quad (9)$$

$$k_R \frac{Z}{E} f(E, 0) \ln \frac{Q_1}{Q_m} = k_R \frac{Z}{E} f(E, 0) \ln \frac{Q_1 2mc^2 \beta^2}{E^2} \quad (10)$$

where $Q_1 \sim 1$ Ry. This function is a non-relativistic approximation since $Q \ll 2mc^2$. It is shown by the solid line in Fig. 2. The GOS is not needed.

- For the second range of Q , use Eq. (6) to calculate numerically $\sigma_2(E)$ for $Q_1 < Q < \infty$ for $E < 10$ keV for Si (see Eq. 2.10 and Fig. 8 in [2]). These integrals were done numerically with the GOS calculated with the method of [19] for the K- and L- electron shells, and with methods described by the ORNL group for the M-shell electrons [28]. Details can be found in [2]. The function is

$$\sigma_2(E) = \int_{Q_1}^{\infty} \sigma(E, Q) dQ = k_R \frac{Z}{E} \int_{Q_1}^{\infty} f(E, Q) \frac{dQ}{Q} \quad (11)$$

The choice of fixed limits for the integral means that the integral is independent of particle speed. $\sigma_2(E)$ is shown by the solid line in Fig. 3.

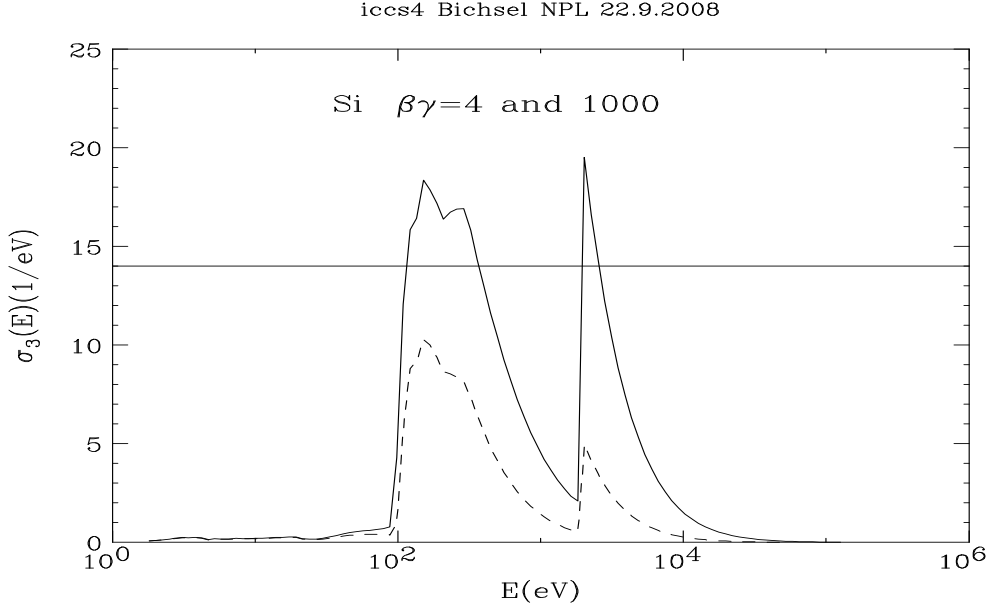


Figure 4: Solid line: third part of B-F cross section, Eq. (14), for $\beta\gamma = 1000$; dashed line: for $\beta\gamma = 4$. Third part of FVP, Eq. (16), is identical. Horizontal line: Rutherford cross section for $Z = 14$ electrons.

- For large values of E (fig. 2 in Fano) $f(E, Q)$ can be approximated by a delta-function (also see fig. 2 in [18]). The approximations given by Eq. 28 in Fano [6] for longitudinal and transverse excitations are used for Eq. (2), now relativistic, resulting in

$$\sigma_3(E) = k_R \frac{Z}{E^2} \left[\frac{1}{1+s} + \frac{s}{1+s} - s(1-\beta^2) \right] \quad (12)$$

with $s = E/2mc^2$, and Q and E are the same. This function is an extension of $\sigma_2(E)$ to larger values of E . It is shown in Fig. 3 as the extension of the solid line beyond $E = 10$ keV. According to the derivation [6] the first term in the square bracket represents longitudinal excitations, the second and third term are due to transverse excitations.

Without the separation we get

$$\sigma_h(E) = k_R \frac{Z}{E^2} [1 - s(1-\beta^2)] \quad (13)$$

which corresponds to the Rutherford cross section, Fig. 3.⁸

⁸See the paragraph above Sect. 2.5 in Fano. The *practical limit* for “large energy loss” E can be seen in Fig. 8 and Eq. (3.4) in [2].

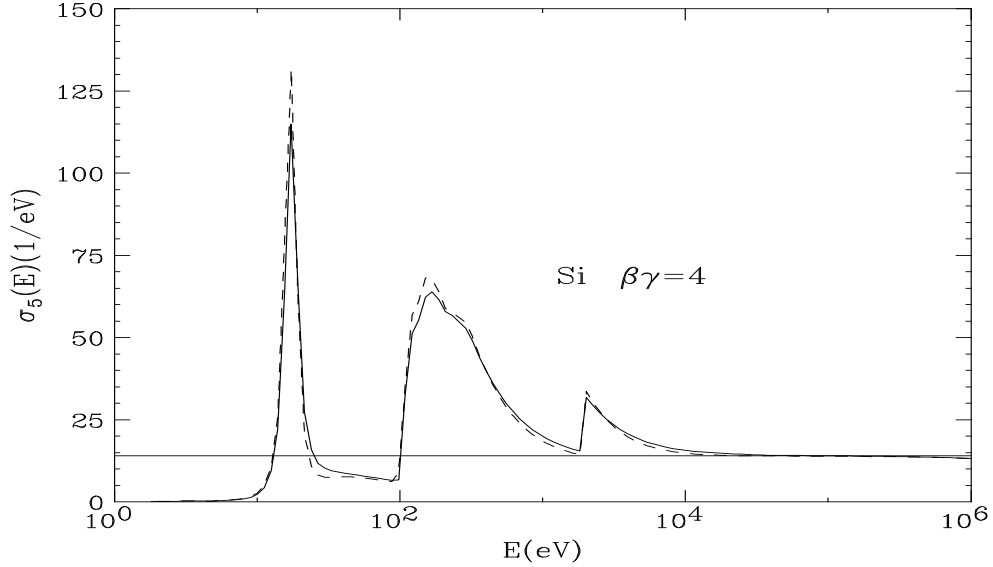


Figure 5: Solid line: total B-F cross section, given by the sum Eq. (15) for $\beta\gamma = 4$. Dashed line: total PAI cross section, Eqs.(16-18). Horizontal line: Rutherford cross section for $Z = 14$ electrons. The functions are multiplied by E^2/k_R or $E^2\beta^2\pi/\alpha$.

- Additional terms are needed for condensed materials [6]. They are related to the collective excitation of many electrons by the passing particle. The dielectric constant $\epsilon(\omega)$ is used to describe these effects ($\hbar\omega$ is equivalent to E). The expression Eq. (14) is Eq. (47) in Fano [6].

$$\sigma_4(E; \beta) = \frac{\alpha}{\beta^2\pi} \frac{\sigma_\gamma(E)}{EZ} \ln[(1 - \beta^2\epsilon_1)^2 + \beta^4\epsilon_2^2]^{-1/2} + \frac{\alpha}{\beta^2\pi} \frac{1}{N\hbar c} \left(\beta^2 - \frac{\epsilon_1}{|\epsilon|^2}\right)\Theta \quad (14)$$

This function is given in Fig. 4 for two particle speeds.

- The total cross section differential in energy loss E is given by Eqs. (10-14)

$$\sigma_5(E; \beta) = \sigma_1(E; \beta) + \{\sigma_2(E) + \sigma_3(E)\} + \sigma_4(E; \beta) \quad (15)$$

It is shown by the solid line in Fig. 5.

2.2 FVP method

The approximation for the GOS used by Allison and Cobb [7] for their method of calculating $\sigma(E; \beta)$ is shown in Fig. 1. The GOS is represented by the horizontal line at $f(E, 0)$ and a delta function at

$Q = E$, i.e. the free electron value of Eq. (5). See the Appendix for details. The collective excitations are represented by Eq. (16) which is the same as Eq. (14) of the B-F method.

The total cross section calculated with the FVP method [7] then is written as

$$\sigma_A(E) = \frac{\alpha}{\beta^2\pi} \frac{\sigma_\gamma(E)}{EZ} \ln[(1 - \beta^2\epsilon_1)^2 + \beta^4\epsilon_2^2]^{-1/2} + \frac{\alpha}{\beta^2\pi} \frac{1}{N\hbar c} (\beta^2 - \frac{\epsilon_1}{|\epsilon|^2})\Theta \quad (16)$$

$$+ \frac{\alpha}{\beta^2\pi} \frac{\sigma_\gamma(E)}{EZ} \ln \frac{2mc^2\beta^2}{E} \quad (17)$$

$$+ \frac{\alpha}{\beta^2\pi} \frac{1}{E^2} \int_0^E \frac{\sigma_\gamma(E')}{Z} dE' \quad (18)$$

Eq. (16) is identical with Eq. (14). Eq. (17) is similar to Eq. (10) with the difference that Q_1 is replaced by $Q_M = 2mc^2\beta^2$. The difference between the two expressions is large, as seen in Fig. 2.

Eq. (18) is given in Fig. 3 by the dashed line. For large energy losses E it is equivalent to the Rutherford cross section and thus is equivalent to Eq. (13), but without the term $s(1 - \beta^2)$. The large differences for $E < 10$ keV compensate those seen in Fig. 2.

The total cross section given by Eqs. (16-18) is shown by the dashed line in Fig. 5. The compensation of the large differences in Figs. 2 and 3 brings σ_5 , Eq.(15), quite close to σ_A , Eqs.(16-18).

2.3 Dependence on particle speed

For large particle speeds $\beta \sim 1$, σ_1 and σ_h of B-F are practically constant, while σ_2 is constant for all β . Only σ_4 will change considerably with γ , as seen in Fig. 4. We see in Fig. 6 that indeed the change in σ_4 is fairly large for large differences in γ , for the range of E where σ_4 is large.

3 Conclusions

The approximation for the GOS shown in Fig. 1 results in the differences shown in Figs. 2 and 3. For the total DCCS, these differences are compensated to a large extent, as seen in Fig. 5. A quantitative description can be given by a comparison of the moments $M_0 = \int \sigma(E) dE$ and $M_1 = \int E \sigma(E) dE$ of the DCCS. This comparison is given for Si in Table 1, derived from Table 1 in [1]. The fractional difference δ of the most probable energy loss Δ_p for a Si layer $x = 8 \mu\text{m}$ is also given. It is about one

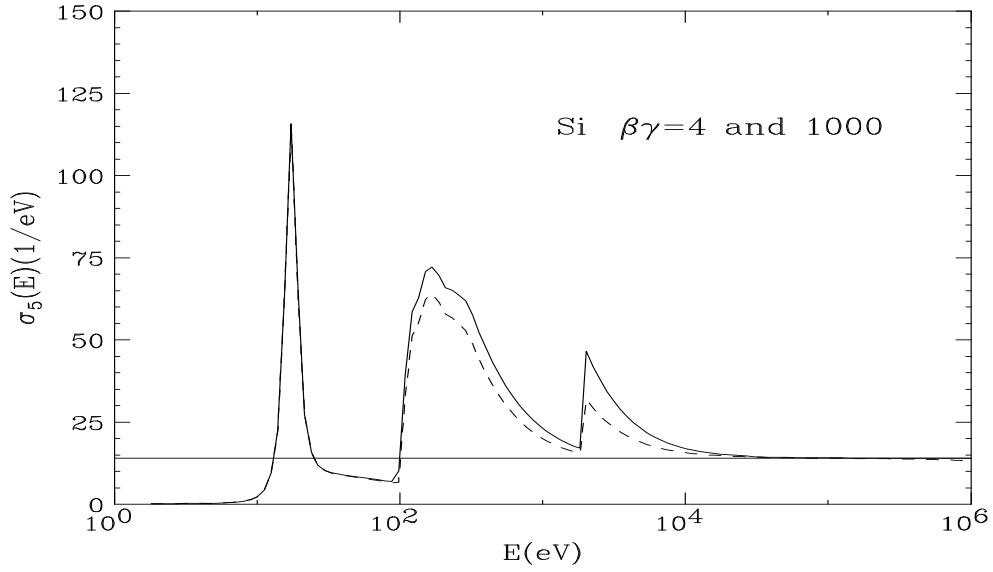


Figure 6: Comparison of the total B-F cross sections, Eq.(14), for $\beta\gamma = 4$, dashed line, and $\beta\gamma = 1000$, solid line.

half of the difference for M_0 . The difference in M_0 may be too large for accurate work and should be explored further, especially for gases. The difference for M_1 is less than 1%.

Table 1. Comparison of M_0 , M_1 and δ_p for B-F and FVP [1].

$\beta\gamma$	M_0			M_1			Δ_p
	B-F	FVP	diff%	B-F	FVP	$\delta\%$	
0.316	30.32	32.78	8.1	2443.7	2465.3	0.9	2.7
1.000	6.729	7.175	6.6	578.3	581.8	0.6	3.5
3.981	3.952	4.189	6.0	386.1	387.9	0.5	3.7
10.000	3.842	4.068	5.9	416.9	418.6	0.4	3.4
100.000	3.842	4.066	5.8	503.8	505.4	0.3	3.2

A The GOS approximation

The approximation of GOS used in [7] can be represented in a primitive fashion as follows.

- In Eq. (9) for σ_1 replace the limit Q_1 by $Q_M = E$. The result is

$$\sigma(E; \beta) = k_R \frac{Z}{E} f(E, 0) \ln \frac{2mc^2 \beta^2}{E} \quad (19)$$

which is equal to Eq. (17). This includes a fraction of σ_2 of Eq. (11).⁹

- For the delta-function at $Q_M = E$ stipulate that all electrons which can be excited by virtual photons with energy E can be considered to be *free electrons* for which the Rutherford cross section can be used. For Eq. (13) we then have

$$Z_{eff} = \int_0^E f(E, 0) dE \quad (20)$$

This results in Eq. (18).

As described in [7] this requirement fulfills the Bethe sum rule (Eq. 27 in Fano)¹⁰

$$\int f(E, Q) dE = 1 \quad (21)$$

The difference in the DCCS seen in Fig. 5 is due to the fact that there is no expression corresponding to Eq. (21) for the integral over Q

$$\int f(E, Q)/Q dQ \quad (22)$$

see Eqs. (2.11,3.4) and figure 8 in [2].

⁹Consider Fig. 2 in Fano. The integral over Q in Eq. (9) for the FVP method extends over the shaded area from $Q_m(E, 0) = E^2/E_M$ to the dashed line $Q = E$, in B-F method to ∞ .

¹⁰With this condition we can expect that M_1 calculated with FVP will be correct within the Bethe approximation (i.e. no shell corrections, Sect. III A in [21]).

References

- [1] *A method to improve tracking and particle identification in TPCs and silicon detectors*, Hans Bichsel, Nucl. Instr. and Meth. **A 562** (2006) 154-197.
- [2] *Stragglings in thin silicon detectors*. Hans Bichsel, Rev. Mod. Phys. **60** (1988) 663.
- [3] *On the energy loss of fast particles by ionization* L. Landau, [Sov.] J. Phys. **VIII** (1944) 201.
- [4] Börsch-Supan, W., 1961, J. Res. Nat. Bur. Stand. **65B** 245.
- [5] *Ueber die Theorie des Stosses zwischen Atomen und elektrisch geladenen Teilchen* E. Fermi, Z. Phys. **29**, 315-327 (1924).; and *Sulla teoria dell'urto tra atomi e corpuscoli elettrici*, E. Fermi, Nuovo Cimento **2**, 143-158 (1925), and H. Bethe, Ann. Phys **5** (1930) 325.
- [6] *Penetration of protons, alpha particles and mesons*. U. Fano, Ann. Rev. Nucl Sci. **13** (1963) 1-66.
- [7] W.W.M. Allison, and J. H. Cobb. Relativistic charged particle identification by energy loss. Ann. Rev. Nucl. Part. Sci. **30** (1980) 253-298.
- [8] *The penetration of atomic particles through matter* Niels Bohr, Dan. Mat. Fys. Medd. **18** no. 8 (1948)(ed.2,1953). Available at <http://www.sdu.dk/Bibliotek/E-hotel/MatFys.aspx>
- [9] *Atomic interaction in penetration phenomena* Aage Bohr, Dan. Mat. Fys. Medd. **24** no. 19 (1948).
- [10] M. Gryzinski, Phys. Rev. **138 A** (1965) 336-358.
- [11] Walske, MC. (1952). The stopping power of K-electrons. Phys. Rev. **88**, 1283-1289.
- [12] Walske, MC. (1956). Stopping power of L-electrons. Phys. Rev. **101**, 940-944.
- [13] K.Sera et al., (1980). Stopping power of M-electrons. Phys. Rev. **A 22**, 2536.
- [14] Bichsel, H. (1983). Stopping power of M-shell electrons for heavy charged particles. Phys. Rev. **A 28**, 1147-1150.

- [15] Inokuti, M. (1971). Inelastic collisions of fast charged particles with atoms and molecules- the Bethe theory revisited. *Rev. Mod. Phys.* **43**, 297-347, and **50**, 23 (1978).
- [16] M Inokuti and Y-K Kim and R L Platzman *Phys Rev* **164** (1967) 55
- [17] *Oscillator-strength moments, ... atoms through strontium*, Inokuti, M., J. L. Dehmer, T. Baer, and J. D. Hanson, *Phys. Rev. A* **23** (1981) 95.
- [18] *Calculation of inner-shell ionization ...*, D. Bote and Fancesc Salvat, *Phys. Rev. A* **77** (2008) 042701
- [19] Manson, ST. (1972). Inelastic collisions of fast charged particles with atoms: ionization of the aluminum L shell, *Phys. Rev. A* **6**, 1013-1024.
- [20] M. Dingfelder, M. Inokuti, *Radiation Protection Dosimetry* **99** (2002) 23-28.
- [21] *Shell corrections in stopping power* H. Bichsel, *Phys. Rev. A* **65** (2002) 052709.
- [22] Lindhard, J., and A. Winther, 1964, *Mat. Fys. Medd. Dan. Vid. Selsk.* **34**, no.4.
- [23] J. Lindhard, *Nucl. Instrum. Methods* **132** (1976) 1.
- [24] S. Segui, M. Dingfelder, J. M. Fernandez and F. Salvat, *J. Phys. B* **35** (2002) 33-53.
- [25] D. Liljequist, *J. Appl. Phys* **57** (1985) 657
- [26] *Manson GOS evalautions* Inokuti, et al., to be selected.
- [27] *Spectral distribution of atomic oscillator strengths.* U. Fano and J. W. Cooper, *Rev. Mod. Phys.* **40** (1968) 441.
- [28] *Inelastic interactions ...* C. J. Tung et al., Report number ORNL-TM-5188 (1976).
- [29] *Radiation energy loss ...* V. M. Grichine, S.S. Sadilov, *Nucl. Instr. and Meth. B* **559** (2003) 26-40.